Please do not adjust margins

Journal of Materials Chemistry C

ARTICLE

Single-Walled Carbon Nanotube/Polystyrene Core-Shell Hybrids: Synthesis and Photoluminescence Properties

Received 00th January 20xx,
Accepted 00th January 20xx

DOI: 10.1039/x0xx00000x

www.rsc.org/

L. Orcin-Chaix,[a,b] G. Trippé-Allard,[a] C. Voisin,[c] H. Okuno,[d] V. Derycke,[b] J.-S. Lauret[a] and S. Campidelli[b,*]

The formation of core-shell structures has permitted to improve greatly the emission properties of inorganic quantum dots. Single-Walled Carbon Nanotubes, thanks to their emission in the near infrared region, are promising materials for optoelectronics. However, the extreme sensitivity of nanotubes to their environment hinders their applications. Thus, the fabrication of tailor-made functional hybrid materials that preserve the optical properties of SWNTs and facilitate their manipulation is extremely important. Here, we describe the synthesis of core-shell nanotube materials made of SWNTs and polystyrene. We developed a two-step strategy that permits to form a stable and homogeneous layer of polymer around the nanotubes by adding first polystyrene *via* the micelle swelling method and then by locking the structure *via* radical polymerisation in micelles of styrene and divinylbenzene. After polymerisation and redispersion, the nanotube hybrids can be easily manipulated in solution; they still exhibited photoluminescence properties both in solution and in the solid state demonstrating that the SWNTs embedded in their polystyrene shell are isolated one from each other.

Introduction

For the last ten years the constant progress made on carbon nanotube chemistry has allowed the full exploitation of the extraordinary properties of these materials. The recent development of sorting techniques, like gradient density ultracentrifugation,[1,2] chromatography,[3-5] polymer wrapping[6,7] or aqueous two phase separations[8,9] permit to separate semiconducting and metallic Single-Walled Carbon Nanotubes (SWNTs) allowing to envision their applications in various domains such as electronics, optoelectronics or quantum information.[10-19] However, still a number of issues remain. One of these issues is related to the structure of nanotubes that are made of surface atoms. The consequences are a large uncontrolled sensitivity to their close environment and an enhanced fragility in comparison to other nanostructures. For instance, the deposition of a dielectric material such as SiO_2 on top of nanotubes induces defects in the nanotube structure[19] while the presence of oxygen and water are responsible of the p-type character of carbon nanotube field effect transistors[20] and of the spectral diffusion and blinking of the photoluminescence.[21] In order to fabricate quantum emitters based on SWNT, the blinking and the spectral diffusion must be suppressed which implies to be able to control the local environment of the nanotubes. Several studies demonstrated that the deposition of polymers such as polystyrene,[22] polymethacrylate[21] on SWNTs or their incorporation in agarose gel[23] permitted to stabilise their light emission. Nevertheless, as efficient as they are, these routes are not suitable to build real devices based on single nanotubes. For instance, such matrices are not compatible with lithography techniques used to build high quality photonic or electronic devices.

One route to take advantage of the protection offered by polymers is to synthesise core/shell nanostructures in which the nanotube is the active core and the polymer, tightly bound to the nanotubes, acts as a protective shell. This strategy is inspired by quantum dots, for which the synthesis of a thick shell around the active core has greatly improved their optical properties: *e.g.* enhanced fluorescence quantum yield and better emission stability.[24]

The encapsulation of carbon nanotubes in shells of surfactants was reported several times over the last 15 years. Initially, it was based on the polymerisation of surfactant molecules pre-organised around the nanotubes by cross-linking either using bifunctional molecules[25,26] or initiated by UV light or radical.[27-29] Alternatively, Chen *et al.*[30] reported formation of Nylon around nanotubes through emulsion polymerisation at the water/surfactant interface. In 2013, we described a completely new method of non-covalent functionalisation of SWNTs which consists of the polymerisation in micelles of porphyrin molecules around the nanotubes.[31] The micelles act as nano-

[a] Laboratoire Aimé Cotton, CNRS, Univ. Paris-Sud, ENS Cachan, Université Paris-Saclay, 91405 Orsay Cedex, France.
[b] LICSEN, NIMBE, CEA, CNRS, Université Paris-Saclay, CEA Saclay 91191 Gif-sur-Yvette Cedex, France. E-mail: stephane.campidelli@cea.fr
[c] Laboratoire Pierre Aigrain, École Normale Supérieure, CNRS, Université Pierre et Marie Curie, Université Paris Diderot, PSL, Sorbonne Paris Cité, Sorbonne Université, 24, rue Lhomond, F-75005 Paris, France.
[d] University Grenoble Alpes, INAC-SP2M, and CEA, INAC-SP2M, LEMMA, F-38000 Grenoble, France.

Electronic Supplementary Information (ESI) available: SEM and AFM images of **SWNT** and **SWNT-PS1** as well as additional images of **SWNT-PS2**, comparison between Raman spectra of the nanotube hybrids. See DOI: 10.1039/x0xx00000x

Please do not adjust margins

Please do not adjust margins

reactors to localise the polymer around the nanotubes. After removing the surfactants, SWNTs embedded in porphyrin polymer shells were obtained; this porphyrin polymer was able to prevent the re-aggregation and allowed the retention of the emission properties of the SWNTs in organic solution and also in the solid state. Later, Nakashima and co-workers adapted the strategy to perform radical polymerisation of acrylamide molecules around SWNTs.[32,33] After polymerisation, the absorption spectra of the nanotubes showed a slight broadening of the transitions; nevertheless the photoluminescence of the nanotubes, dispersed in water, was still observed.

The aim of this work is to synthesise emitting core-shell nanotube hybrids that can be easily manipulated in solution. In order to form such a robust and thick shell of polymer around the nanotubes, we decided first to introduce a large amount of polystyrene on the nanotube sidewalls and then, in a second time, to cross-link the structure *via* radical polymerisation of styrene and divinylbenzene. Compared to polyfluorene, for example, polystyrene does not wrap efficiently around nanotubes. Therefore the second step was performed to avoid the redissolution of the first layer of polystyrene and ensure the stability of the organic shell around the nanotubes

The two steps of functionalisation were based on the micelle swelling method.[34,35] The nanotubes were first dispersed in surfactant solutions and then polystyrene dissolved in dichloromethane was non-covalently adsorbed on the nanotube surfaces. In a second time and in order to lock the structure, styrene and divinylbenzene monomers were introduced in the micelles and were polymerised (see Chart 1). The core/shell structures were characterised by scanning and transmission electron microscopy (TEM, SEM), atomic force microscopy (AFM) and thermogravimetric analysis (TGA). In particular the width of the shell is investigated as well as its homogeneity. Moreover, the effect of the shell on the optical properties of the nanotubes was investigated by Raman spectroscopy and the photoluminescence properties were studied in solution and in the solid state.

Results and discussion

The preparation of the polystyrene/nanotube hybrids is described in Chart 1. First HiP_{CO} SWNTs were dispersed in 2 wt % SDS solution (1h30, 20 W sonic tip in an ice bath) and centrifuged at 150 000 g for 1h. The supernatant was separated and used for the micelle swelling functionalisation. We performed the functionalisation in two steps; the first step consisted of the adsorption of commercial polystyrene (PS) polymer (Aldrich, average M_w 35 000) dissolved in

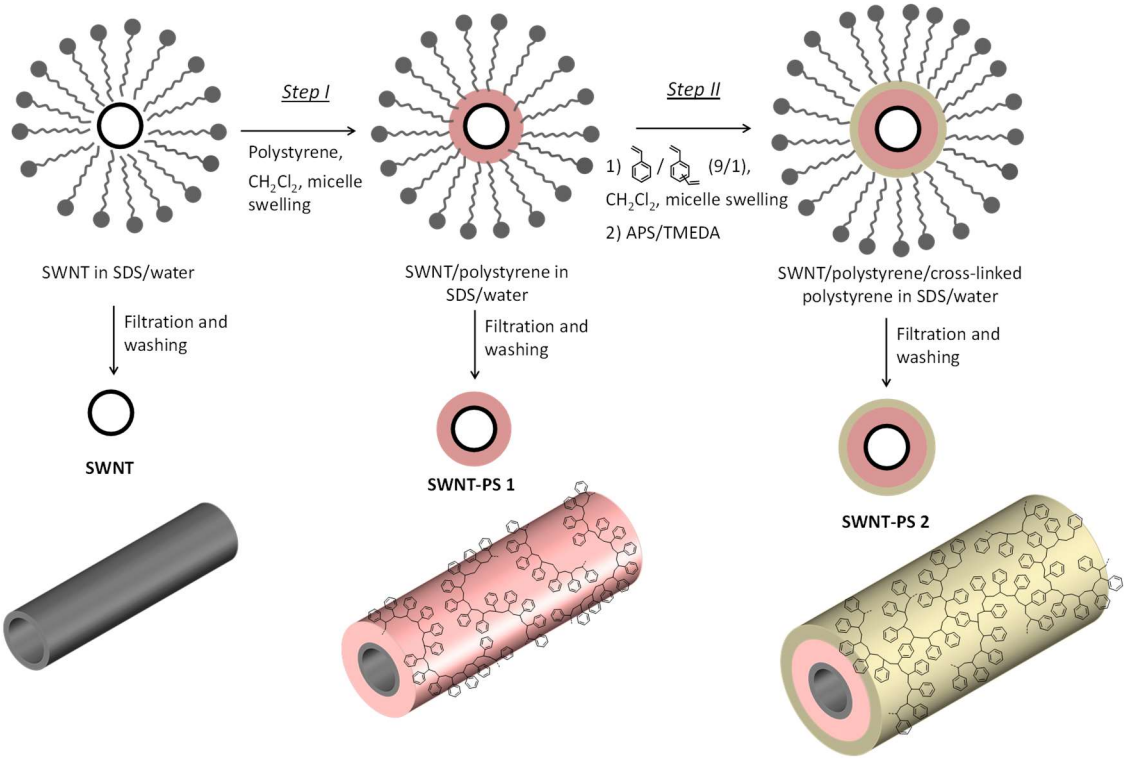


Chart 1. Functionalisation of SWNTs. (Step I): polystyrene in CH_2Cl_2 was introduced using the micelle swelling method on the nanotube sidewalls; HiP_{CO} SWNTs were initially dispersed in sodium dodecylsulfate (SDS) 2wt % in water. (Step II): a mixture of styrene and divinylbenzene (DVB) in CH_2Cl_2 was introduced in the micelles and ammonium persulfate (APS) and *N*,*N*,*N'*,*N'*-tetramethylethylenediamine (TMEDA) were introduced to the nanotube solution to initiate the polymerisation. After Steps I and II, the nanotubes were purified by filtration and extensive washing and were redispersed in solvents for analyses. The bottom part of the figure shows the representation of different nanotube derivatives **SWNT**, **SWNT-PS1** and **SWNT-PS2**.

 This journal is © The Royal Society of Chemistry 20xx

Please do not adjust margins

Journal of Materials Chemistry C

ARTICLE

dichloromethane (1 mg/mL) on the nanotubes *via* the micelle swelling method.[35] This first step aimed at forming a protective layer on the nanotubes; the procedure was repeated three times in total to ensure that all the nanotubes are covered with the polymer. The second step consisted of the formation of cross-linked polystyrene around the nanotubes to improve the robustness of the PS shell: a mixture of styrene and divinylbenzene (DVB) (9/1 v/v) in dichloromethane was introduced in the micelles *via* the micelle swelling method[35] and then the radical initiators (ammonium persulfate – APS and *N*,*N*,*N'*,*N'*-tetramethylethylenediamine – TMEDA) were added. The reaction was stirred at room temperature for 48h. After the reaction, the nanotubes solution were filtered on a 0.2 µm PTFE membrane and washed with water, ethanol, acetone and THF to remove the surfactants, the reagents and the polymers not bound to the nanotubes. The nanotubes-polystyrene hybrids **SWNT-PS2** were redispersed in THF and used for the characterisation. In order to produce reference samples, the initial solution of **SWNT** and the nanotubes-polystyrene hybrids **SWNT-PS1** (obtained after the first micelle swelling step with polystyrene) received the same purification treatment: they were filtered through a 0.2 µm PTFE membrane and washed with water, ethanol, acetone and THF and then redispersed in THF. It is worth mentioning that the suspensions obtained in THF for **SWNT** and **SWNT-PS1** were not stable compared to those of **SWNT-PS2** and rapidly flocculated.

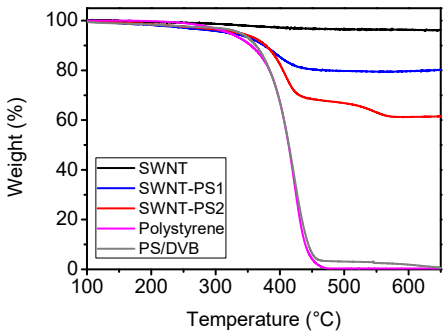


Fig. 1 Thermal decomposition (TGA) of **SWNT** (black), **SWNT-PS1** (blue), **SWNT-PS2** (red), commercial polystyrene from Aldrich (magenta) and PS/DVB (grey) at 10°C/min under nitrogen.

The nanotubes hybrids were first analysed by TGA; the thermograms of pristine and functionalised SWNTs and the one of polystyrene used as reference are presented in Fig. 1. At 600°C, under N_2, **SWNT** exhibit a negligible loss of weight of 3.5% while at the same temperature, polystyrene is completely decomposed. The thermograms of **SWNT-PS1** and **SWNT-PS2** clearly show the presence of polystyrene on the nanotubes. From the TGA curves the total amount of polystyrene was estimated to *ca* 17% and 36% for **SWNT-PS1** and **SWNT-PS2**, respectively. It is interesting to notice the difference between the two hybrids: first, the polystyrene in **SWNT-PS2** shows degradation in two steps, both correspond to the degradation of polystyrene but the second step can be attributed to the cross-linked part of the polymer.[36] Secondly, **SWNT-PS2** contains almost two times more polystyrene than **SWNT-PS1** (between 300 and 475°C, the loss of weight is *ca.* 17% for **SWNT-PS1** while it is of *ca.* 29% for **SWNT-PS2**). This is due to a better preservation of the first layer of polystyrene from the dissolution during the work-up (filtration and washing with acetone and THF) by the second cross-linked polymer layer. This observation points out the important role of the polymerisation step in the stabilisation of the structure.

IR spectra of a mixture of styrene/DVB, of the polystyrene/DVB synthesized as reference and of **SWNT-PS2** are presented in Fig. S1. The spectra of nanotube derivatives are quite difficult to interpret since SWNTs exhibit generally a broad and featureless absorption. However, in the 2800-3100 cm^{-1} region, it is interesting to note the presence of the stretching band due to sp^3 C-H in **SWNT-PS2**.

The dispersion and the morphology of the nanotubes hybrids were studied by microscopy techniques (AFM, TEM and SEM). The AFM and SEM images of **SWNT-PS2**, deposited on Si/SiO_2 substrates, taken at different magnification (Fig. 2a-b and 2g-h) show that the polymer is located around the nanotubes and that there is no free polystyrene on the surface. By comparison, SEM images of **SWNT-PS1** show the presence of polymers both on the nanotubes and on the surface (Fig. S2); it indicates that the polystyrene shell around **SWNT-PS1** is not stable and again it highlights the ability of the second polystyrene layer to lock the structure. In order to have a better insight on the structure of the different objects, we performed statistics on the average diameters of **SWNT**, **SWNT-PS1** and **SWNT-PS2** (Fig. 2d). The top part of Fig. 2d shows that the diameters of **SWNT-PS2** samples are relatively homogeneous and centered around 4 nm conversely to those of **SWNT** and **SWNT-PS1** (see Fig. S3 for AFM images of **SWNT** and **SWNT-PS1**). The distribution of diameter of **SWNT** (Fig. 2d – bottom part) is relatively inhomogeneous; it is obvious that untreated SWNTs will re-aggregate quickly in solution when the surfactant shell is removed. The observation of such large dispersion in the measurement of diameter is the signature of the presence of bundles. Moreover, the fact that **SWNT-PS1** exhibits also large diameter dispersions (Fig. 2d – middle part)

This journal is © The Royal Society of Chemistry 20xx

Journal of Materials Chemistry C

ARTICLE

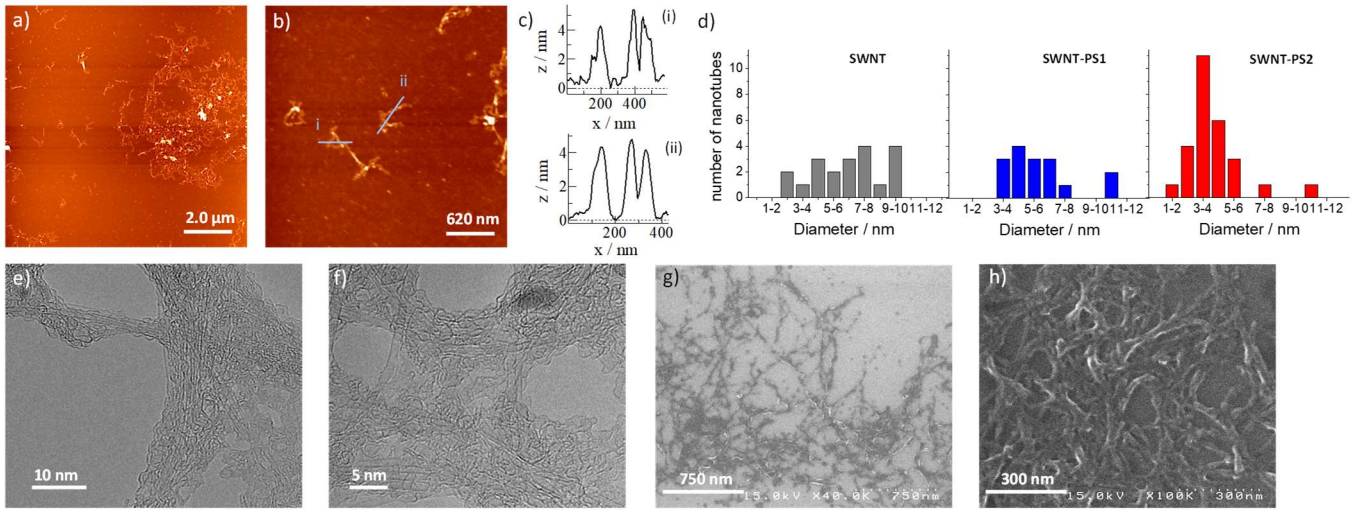


Fig. 2 AFM image of **SWNT-PS2** deposited from THF on Si/SiO_2 substrates: a) at low magnification and b) at higher magnification; c) cross-section corresponding to the blue lines on image (b); d) statistics on the average diameters estimated by AFM of **SWNT-PS2** (in red) **SWNT-PS1** (in blue), **SWNT** (in dark grey); e-f) TEM images of **SWNT-PS2** deposited from THF on Lacey-carbon grids; g-h) SEM image of **SWNT-PS2** deposited from THF on Si/SiO_2 substrates. The presence of the polymer around the nanotubes is clearly observable on the TEM and SEM images.

suggests that the non-cross-linked polystyrene shell is unstable that leads to re-aggregation of nanotubes when they are redispersed in the organic solvent. The difference of stability between **SWNT-PS1** and **SWNT-PS2** in solution can also be directly observed by the experimentalist since the dispersion of **SWNT-PS1** in THF tends to flocculate few minutes after their preparation while suspension of **SWNT-PS2** are stable for days. Therefore, we can conclude that the layer of cross-linked polystyrene permits to avoid the re-aggregation of the nanotubes. The diameter distribution of **SWNT-PS2** is centered on 4 nm. The mean diameter of HiP_{CO} nanotubes being ~1 nm, the thickness of the polystyrene layer must be around 1.5 nm on the nanotubes which is still very thin. Finally, **SWNT-PS1** and **SWNT-PS2** were observed by TEM (Fig. 2e-f and Fig. S4). The micrographs show that the nanotubes are covered by an amorphous layer of polystyrene material as it was suggested from AFM and SEM images. From the images, we observed that the amount of polystyrene around the nanotubes was lower **SWNT-PS1** than for **SWNT-PS2**. In particular, we found a larger amount of nanotubes without polystyrene in the case of **SWNT-PS1**. Unfortunately, because of the aggregation of the materials during the drying of the TEM grids, the analyses of the images did not permit to confirm the thickness of the coverage deduced from AFM.

The optical properties of the nanotube-based materials were investigated by Raman and photoluminescence excitation (PLE) spectroscopy. The Raman spectra of **SWNT**, **SWNT-PS1** and **SWNT-PS2** recorded after excitation at 532 nm on solid samples (buckypapers) are presented in Fig. 3a; the spectra show only small differences between pristine and functionalised SWNTs in the G-band and the RBM region. The apparent broadening of the G-band for **SWNT** is due to the aggregation of the bare nanotubes compared to the hybrid materials (Fig. S5). Indeed, it is known that the presence of bundles influences the Raman spectra of SWNTs and in particular the intensity and position of the RBM signals as well as the width of the peaks.[37,38] We compared the intensity of the D- and G-bands for **SWNT** and **SWNT-PS2**; very similar ratio were found (D/G_{SWNT} = 0.20 and $D/G_{SWNT\text{-}PS2}$ = 0.19) showing that the polymerisation does not significantly affect the integrity of the nanotubes.

The optical properties of the nanotube hybrids were studied by absorption and photoluminescence excitation (PLE) spectroscopies. Fig. 3b displays the absorption spectra of **SWNT**, **SWNT-PS1** and **SWNT-PS2** dispersed in SDS. The spectra show the characteristic lines of HiP_{CO} nanotubes indicating that the functionalisation process keeps intact the optical properties of nanotubes.[39] Indeed, in the 1000 nm – 1300 nm spectral range one can observe the S_{11} transitions of the different chiralities of the semiconducting nanotubes contained in the sample. Likewise, the S_{22} lines and the M_{11} lines of metallic nanotubes appear in the 500 nm – 900 nm spectral range.[40]

This journal is © The Royal Society of Chemistry 20xx

Please do not adjust margins

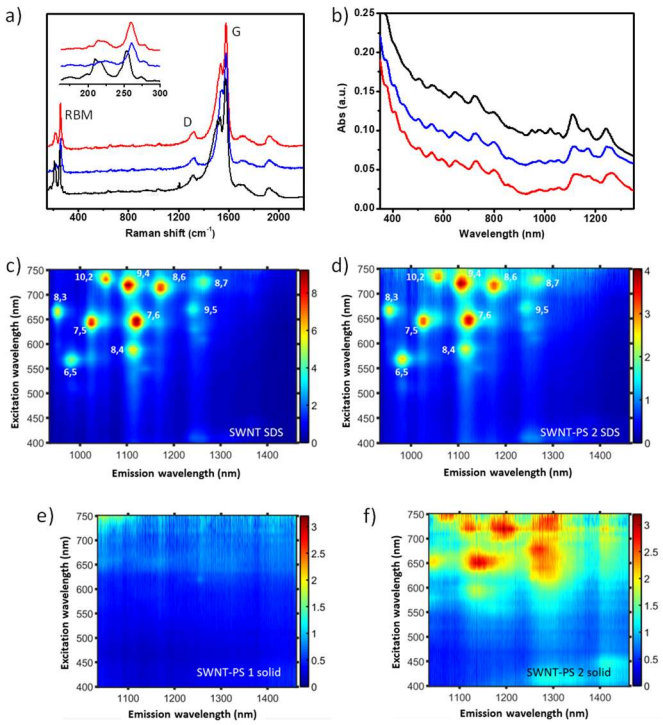


Fig. 3 a) Raman spectra of **SWNT** (black), **SWNT-PS1** (blue) and **SWNT-PS2** (red) recorded at λ_{exc} = 532 nm on solid samples (buckypapers); in inset are shown the RBM modes of **SWNT**, **SWNT-PS1** and **SWNT-PS2**. b) UV-Vis-NIR absorption spectrum of **SWNT** (black), **SWNT-PS1** (blue) and **SWNT-PS2** (red) dispersed in 2 wt % SDS solution; c) PLE maps of **SWNT** dispersed in 2 wt % SDS solution; d) PLE maps of **SWNT-PS2** dispersed in 2 wt % SDS solution; e) PLE maps of a film of **SWNT-PS1** on PTFE membrane; f) PLE maps of a film of **SWNT-PS2** on PTFE membrane.

Fig. 3c-d shows the PLE spectra of **SWNT** and **SWNT-PS2** in suspension in SDS. Again, the PLE resonance characteristic of HiP_{CO} nanotubes can be observed on both samples.[41] The comparison of the fluorescence amplitudes is not straightforward. Indeed, during the functionalisation process the pH of the solution is modified due to the addition of TMEDA. The fluorescence of nanotubes is known to be strongly dependent on the pH.[42] Moreover, the effect is also diameter dependent which complicates the analysis. Nevertheless, the level of fluorescence of **SWNT-PS2** is compatible with the preservation of the pristine properties of nanotubes along the chemical functionalisation. It is worth mentioning that even if **SWNT-PS2** can be solubilised in THF; optical investigations cannot be performed on such suspensions since THF exhibits strong absorption lines in the near infrared. Finally, the fluorescence properties of the hybrid materials **SWNT-PS1** and **SWNT-PS2** were studied in the solid state: Fig. 3e-f displays the PLE maps of films of **SWNT-PS1** and **SWNT-PS2** on PTFE membranes. While **SWNT-PS1** shows no fluorescence, the film of **SWNT-PS2** still exhibits luminescence signals. The low signal to noise ratio of Fig. 3f, that may have several origins, prevents a precise analysis of the differences between spectra in solution (Fig. 3d) and on films (Fig. 3f). Nevertheless, we can draw some comments. First, these experiments are performed on dense films where nanotubes may undergo some strains. This can explain the broadening of the PLE lines and loss in signal to noise ratio. Likewise, although it is difficult to evaluate precisely the number of nanotubes in the excitation volume, it has to be much smaller on films leading to less PL signal. Finally, energy transfer between nanotubes in the film cannot be excluded. Energy transfer from semiconducting to metallic nanotubes can induce a decrease of the PL signal and transfer from small diameter nanotubes to larger ones could explain the apparent change in the PL intensity ratios. Nevertheless, the total absence of luminescence on films of **SWNT-PS1** show that the strategy that we develop: 1) wrapping of polystyrene on the nanotube surfaces and 2) formation of a cross-linked polymer to "lock" the structure permit to better preserve the isolation of the nanotubes. Finally, ensemble measurements are sensitive to averaging effects. Therefore, experiments at the single core-shell are mandatory to conclude on the total protection of the nanotube. These experiments are under progress, but they are far beyond the scope of the present paper.

Conclusion

We described the synthesis of core-shell nanotube materials made of HiP_{CO} SWNTs and polystyrene. We adopt a strategy in two steps in which we add first a large amount of polystyrene on the nanotubes sidewalls to ensure a good protection against the environment and then we performed a radical polymerisation with styrene and divinylbenzene to cross-link the structure and improve the interaction between the polymer and the nanotube. The nanotube/polystyrene hybrids were characterised by a combination of techniques including thermogravimetry, SEM and AFM microscopies, and by optical spectroscopies (Raman, absorption and PLE). AFM analyses demonstrated that the nanotube hybrids containing a double shell of polymer **SWNT-PS2** exhibited a narrow diameter distribution showing that the initial individualisation of the nanotubes was better preserved in the solid state with this strategy compared to the simple wrapping with polystyrene. The same conclusion was drawn from the PLE experiments performed in the solid state. Therefore a double layer of polystyrene on SWNTs enhances the solubility of the hybrids in organic solvent and limits the re-aggregation of the nanotubes. So, we are able to deposit nanotubes individually embedded in a polymer matrix and we are now studying their properties at the single nanotube level. Such core-shell carbon nanotube hybrids exhibiting photoluminescence in the infrared may have important implication for future optoelectronic devices.

Experimental section

Techniques. Raman Spectra were recorded on a Horiba-Jobin Yvon LabRAM ARAMIS spectrometer with excitation at 532

Please do not adjust margins

Please do not adjust margins

nm. The thermogravimetric analyses were performed with a TGA Q50 (TA Instruments) at 10 °C/min under N_2. For the AFM and SEM analyses: nanotube hybrids dispersed in THF were drop-casted on freshly cleaned Si/SiO_2 surfaces and immediately dried by N_2 blow drying. The samples were investigated with a Veeco Dimension 3100 AFM or a Multimode AFM equipped with Nanoscope IIIa controllers and with a Hitachi S-4500 Scanning Electron Microscope. Optical absorption spectroscopy is performed with a lambda900 UV/Vis/NIR spectrophotometer (Perkin Elmer). A 1000 W Xenon lamp filtered with a monochromator is used as an excitation source for photoluminescence excitation experiments. The luminescence is then analyzed with an Acton SP2500i spectrometer equipped with an OMAV InGaAs diode array.

Materials. Chemicals were purchased from Aldrich and were used as received. Solvents were purchased form Aldrich, Thermo Fisher Scientific or SDS Carlo Erba and were used as received. The stabilizing agents in the styrene and divinylbenzene monomers were removed by distillation for styrene and column chromatography on alumina for DVB. HiP_{CO} SWNTs were purchased from Carbon Nanotechnologies, Inc. (CNI). Polystyrene average M_w 35,000 (Aldrich 331651) was used for the first micelle swelling step.

Synthesis. Preparation of the initial SWNT solution. The solution of HiP_{CO} SWNTs was prepared by sonicating the nanotubes at 1 mg/mL in SDS (2 wt %) solution for 1.5 h with an ultrasonic tip Sonics Vibra-Cell™ VCX-500 followed by ultracentrifugation at 150 000 g for 1 h. The supernatant was recovered and used for the different reactions. The reference solution of nanotubes called **SWNT** was prepared by filtration of the nanotube solution in SDS through a 0.2 µm PTFE membrane followed by extensive washing with water, ethanol, acetone and THF; then they were redispersed in THF.

SWNT-PS1. 100 µL of polystyrene solution (1 mg/mL) in CH_2Cl_2 was added to SWNTs in SDS (4 mL). The mixture was sonicated for 5 min. at the maximum power of a sonic bath (2.5 liters Fisherbrand, model FB 11201), then at 50% of the maximum power of the sonic bath for 15 min. to obtain a clear solution. This step (addition and sonication) was repeated three times in total. After reaction the nanotubes were filtered through a 0.2 µm PTFE membrane, washed with water, ethanol, acetone and then THF. **SWNT-PS1** were redispersed in THF or in SDS solution with sonic bath or ultrasonic tip.

SWNT-PS2. 100 µL of a solution of styrene/DVB (9/1) (1 mg/mL) in CH_2Cl_2 was added to **SWNT-PS1** (4 mL). The mixture was sonicated for 5 min. at the maximum power of a sonic bath, then at 50% of the maximum power of the sonic bath for 15 min. to obtain a clear solution. A 20 wt % aqueous solution of ammonium persulfate (30 µL) and 4 drops of *N,N,N′,N′*-tetramethylethylenediamine (TMEDA) were added to the aqueous nanotubes solution. The mixture was stirred for one night. After reaction the nanotubes were filtered through a 0.2 µm PTFE membrane, washed with water, ethanol, acetone and then THF. **SWNT-PS2** were redispersed in THF or in SDS solution with sonic bath or ultrasonic tip.

PS/DVB. 500 µL of a solution of styrene/DVB (9/1) was added to a 2 wt % SDS solution (20 mL). The milky suspension was sonicated for 15 min. at the maximum power of a sonic bath. A 20 wt % aqueous solution of ammonium persulfate (100 µL) and TMEDA (100 µL) were added to the suspension. The mixture was stirred for 2 days at room temperature, the suspension turned to slightly yellow transparent. Methanol (50 mL) was added to precipitate the polystyrene and the suspension was filtered through a 0.2 µm PTFE membrane, washed with methanol and dried under vacuum.

Conflicts of interest

There are no conflicts to declare.

Acknowledgements

This work was partly funded by the JST-ANR program TMOL "Molecular Technology" project MECANO (ANR-14-JTIC-0002-01) and by a public grant overseen by the French National Research Agency (ANR) as part of the "Investissements d'Avenir" program (Labex NanoSaclay, reference: ANR-10-LABX-0035). J.-S. Lauret is member of "Institut Universitaire de France".

Note and references

1 M. S. Arnold, A. A. Grenn, J. F. Hulvat, S. I. Stupp and M. C. Hersam, *Nat. Nanotechnol.*, 2006, **1**, 60-65.
2 S. Ghosh, S. M. Bachilo and R. B. Weisman, *Nat. Nanotechnol.*, 2010, **5**, 443-450.
3 T. Tanaka, H. Jin, Y. Miyata and H. Kataura, *Appl. Phys. Express*, 2008, **1**, 114001
4 H. Liu, D. Nishide, T. Tanaka and H. Kataura, *Nat. Commun.*, 2011, **2**, 309
5 X. Tu, S. Manohar, A. Jagota and M. Zheng, *Nature*, 2009, **460**, 250-253.
6 A. Nish, J.-Y. Hwang, J. Doig and R. J. Nicholas, *Nat. Nanotechnol.*, 2007, **2**, 640-646.
7 F. Chen, B. Wang, Y. Chen and L. J. Li, *Nano Lett.*, 2007, **7**, 3013-3017.
8 C. Y. Khripin, J. A. Fagan and M. Zheng, *J. Am. Chem. Soc.*, 2013, **135**, 6822-6825.
9 J. A. Fagan, E. H. Hároz, R. Ihly, H. Gui, J. L. Blackburn, J. R. Simpson, S. Lam, A. R. Hight Walker, S. K. Doorn and M. Zheng, *ACS Nano*, 2015, **9**, 5377-5390.
10 P. Avouris, Z. Chen and V. Perebeinos, *Nat. Nanotechnol.*, 2007, **2**, 605-615.
11 P. Avouris, M. Freitag and V. Perebeinos, *Nat. Photonics*, 2008, **2**, 341-350.
12 K. Dirian, M. A. Herranz, G. Katsukis, J. Malig, L. Rodríguez-Pérez, C. Romero-Nieto, V. Strauss, N. Martín and D. M. Guldi, *Chem. Sci.*, 2013, **4**, 4335-4353.
13 R. D. Costa, F. Lodermeyer, R. Casillas and D. M. Guldi, *Energy Environ. Sci.*, 2014, **7**, 1281-1296.
14 T. Lei, I. Pochorovski and Z. Bao, *Acc. Chem. Res.*, 2017, **50**, 1096-1104.
15 M. M. Shulaker, G. Hills, R. S. Park, R. T. Howe, K. Saraswat, P. H. S. Wong and S. Mitra, *Nature*, 2017, **547**, 74-78.
16 A. Hogele, C. Galland, M. Winger and A. Imamoglu, *Phys. Rev. Lett.*, 2008, **100**, 217401

 This journal is © The Royal Society of Chemistry 20xx

Please do not adjust margins

Please do not adjust margins

17 A. Jeantet, Y. Chassagneux, C. Raynaud, P. Roussignol, J.-S. Lauret, B. Besga, J. Estève, J. Reichel and C. Voisin, *Phys. Rev. Lett.*, 2016, **116**, 247402
18 S. Khasminskaya, F. Pyatkov, K. Slowik, S. Ferrari, O. Kahl, V. Kovalyuk, P. Rath, A. Vetter, F. Hennrich, M. M. Kappes, G. Gol'tsman, A. Korneev, C. Rockstuhl, R. Krupke and W. H. P. Pernice, *Nat. Photonics*, 2016, **10**, 727-732.
19 X. Ma, N. F. Hartmann, J. K. S. Baldwin, S. K. Doorn and H. Htoon, *Nat. Nanotechnol.*, 2015, **10**, 671-676.
20 C. M. Aguirre, P. L. Levesque, M. Paillet, F. Lapointe, B. C. Saint-Antoine, P. Desjardins and R. Martel, *Adv. Mater.*, 2009, **21**, 3087-3091.
21 N. Ai, W. Walden-Newman, Q. Song, S. Kalliakos and S. Strauf, *ACS Nano*, 2011, **5**, 2664-2670.
22 W. Walden-Newman, I. Sarpkaya and S. Strauf, *Nano Lett.*, 2012, **12**, 1934-1941.
23 L. Cognet, D. A. Tsyboulski, J.-D. R. Rocha, C. D. Doyle, J. M. Tour and R. B. Weisman, *Science*, 2007, **316**, 1465-1468.
24 P. Reiss, M. Protière and L. Li, *Small*, 2009, **5**, 154-168.
25 Y. Kang and T. A. Taton, *J. Am. Chem. Soc.*, 2003, **125**, 5650-5651.
26 R. Wang, P. Cherukuri, J. G. Duque, T. K. Leeuw, M. K. Lackey, C. H. Moran, V. C. Moore, J. L. Conyers, R. E. Smalley, H. K. Schmidt, R. B. Weisman and P. S. Engel, *Carbon*, 2007, **45**, 2388-2393.
27 C. Thauvin, S. Rickling, P. Schultz, H. Célia, S. Meunier and C. Mioskowski, *Nat. Nanotechnol.*, 2008, **3**, 743-748.
28 C. Thauvin, A. Perino, E. Contal, E. Morin, P. Schultz, S. Meunier and A. Wagner, *J. Phys. Chem. C*, 2011, **115**, 7319-7322.
29 T. H. Kim, C. Doe, S. R. Kline and S.-M. Choi, *Adv. Mater.*, 2007, **19**, 929-933.
30 W.-C. Chen, R. K. Wang and K. J. Ziegler, *ACS Appl. Mater. Interfaces*, 2009, **1**, 1821-1826.
31 G. Clavé, G. Delport, C. Roquelet, J.-S. Lauret, E. Deleporte, F. Vialla, B. Langlois, R. Parret, C. Voisin, P. Roussignol, B. Jousselme, A. Gloter, O. Stephan, A. Filoramo, V. Derycke and S. Campidelli, *Chem. Mater.*, 2013, **25**, 2700-2707.
32 Y. Tsutsumi, T. Fujigaya and N. Nakashima, *RSC Adv.*, 2014, **4**, 6318-6323.
33 Y. Tsutsumi, T. Fujigaya and N. Nakashima, *Chem. Lett.*, 2016, **45**, 274-276.
34 R. K. Wang, W.-C. Chen, D. S. Campos and K. J. Ziegler, *J. Am. Chem. Soc.*, 2008, **130**, 16330-16337.
35 C. Roquelet, J.-S. Lauret, V. Alain-Rizzo, C. Voisin, R. Fleurier, M. Delarue, D. Garrot, A. Loiseau, P. Roussignol, J. A. Delaire and E. Deleporte, *ChemPhysChem*, 2010, **11**, 1667-1672.
36 M. Fathy, T. A. Moghny, A. E. Awadallah and A.-H. A. A. El-Ballihi, *Int. J. Mod. Org. Chem.*, 2013, **2**, 67-80.
37 D. A. Heller, P. W. Barone, J. P. Swanson, R. M. Mayrhofer and M. S. Strano, *J. Phys. Chem. B*, 2004, **105**, 6905-6909.
38 L. M. Ericson and P. E. Pehrsson, *J. Phys. Chem. B*, 2005, **109**, 20276-20280.
39 M. J. O'Connell, S. M. Bachilo, C. B. Huffman, V. C. Moore, M. S. Strano, E. H. Haroz, K. L. Rialon, P. J. Boul, W. H. Noon, C. Kittrell, J. Ma, R. H. Hauge, R. B. Weisman and R. E. Smalley, *Science*, 2002, **297**, 593-596.
40 M. A. Hamon, M. E. Itkis, S. Niyogi, T. Alvaraez, C. Kuper, M. Menon and R. C. Haddon, *J. Am. Chem. Soc.*, 2001, **123**, 11292-11293.
41 S. M. Bachilo, M. S. Strano, C. Kittrell, R. H. Hauge, R. E. Smalley and R. B. Weisman, *Science*, 2002, **298**, 2361-2366.
42 J. G. Duque, L. Cognet, A. N. G. Parra-Vasquez, N. Nicholas, H. K. Schmidt and M. Pasquali, *J. Am. Chem. Soc.*, 2008, **130**, 2626-2633.

This journal is © The Royal Society of Chemistry 20xx

Please do not adjust margins